A Collagen Droplet Platform for Screening Malignant Peripheral Nerve Sheath Tumors

A THESIS
SUBMITTED TO THE FACULTY OF THE
UNIVERSITY OF MINNESOTA
BY

Eric J. Conniff

IN PARTIAL FUFILLMENT OF THE
REQUIREMENTSFOR THE DEGREE OF
MASTER OF SCIENCE

David K. Wood., Advisor

June 2022

ACKNOWLEDGEMENTS

Thank you to all my classmates, the Department of Biomedical Engineering, and the professors. You are all truly inspirational in your depth of knowledge and vigor for the sciences.

The entire Wood Lab made each day enjoyable. I would have never imagined a group of individuals so vulnerable, honest, and kind would welcome me into lab with open arms.

Thank you to Heather Bomberger, Katie Cummins, and Ali Crampton. You have all been amazing friends and mentors, in and out of the lab. I could not have finished, nor would have started this without you.

My advisor, David Wood, provided an environment for me to grow, and taught me invaluable lessons that were painful to learn; and for that, I am forever grateful.

I would like to thank my friends and family who were always available when needed; I appreciate it. Most importantly, my parents, without your unwavering support and belief in me, none of this would have been possible.

ABSRACT

The services of monolayer culture in probing underlying mechanisms around cancer cell biology are extensive and have resulted in novel findings that are too numerous to reference in this paper alone. Rather, broadly speaking, 2D has provided a cornerstone in understanding and exploration of high-throughput pharmacological screens, cellular level imaging, methods of studying metastasis, response to chemotherapy agents, and a great deal more. However, recent research in the field of cancer biology demands us to consider the TME, and to supplement current 2D models by migrating towards 3D methodologies. Improved development of 3D platforms and their further integration into the realm of cancer biology is vital for continued scientific progress of the field. Herein, we present the advancement and novel application of a microfluidic-based 3D collagen droplet platform for utilization with *ex vivo* PDX MPNSTs. The platform is then utilized for a single and dual drug screen to probe for potential future therapeutic agents based on cellular viability over time. We culminate these studies by presenting a repository of *ex vivo* PDX MPNSTs across multiple research organizations.

TABLE OF CONTENTS

LIST OF FIGURES

CHAPTER 1

3D Cell Culture Platforms

Section 1.1 – Importance of a High-Quality Culture System

Historically, high-throughput (HT) studies have employed two-dimensional (2D) cell culture methods as they provide an accessible and reproducible model capable of performing HT cell-based assays. Furthermore, the impact and significance of 2D and spheroid cultures regarding their groundbreaking findings on cell-to-cell interactions, and the influence of matrices cannot be understated (Sutherland 1971). However, traditional 2D culture tends to lack the cell-matrix interactions, biomechanical cues, and native tissue architectures presented *in vivo*, ultimately limiting their ability to meaningfully predict cellular behavior (Gupta 2016). These artifacts caused by 2D culture extend beyond cell morphology (Antoni 2015) and into fundamental cell characteristics including varied proliferation rates (Gupta 2016) and cytokine profiles (Baker 2012). By minimizing these systemic artifacts, 3D platforms show increased predictive power and improved functional utility when screening for therapeutic efficacy.

This enhanced capability to screen pharmaceuticals and more accurately predict diseased behavior can prevent repetitive downstream testing in preclinical models, helping to conserve valuable time and resources. Improving the drug safety system and increasing the efficiency of the drug screening process, as well as reducing animal use for *in vivo* studies, will require novel, well-designed 3D test systems. As better systems come online and processed sample throughput increases, new challenges, such as data management and image analysis, will require new automation strategies to streamline operations. Emerging 3D platforms based around spheroids, microcarriers, and various hydrogels hybrids have begun to cross into mainstream use. However, many of these platforms are currently being deployed to explore niche areas and/or lack the consistency and reliability for general mass adoption. Automation of these protocols will require investments in machinery and supporting architecture to increase their potential for broad expansion.

Assessing efficacy, toxicity, and off-target impacts of pharmaceuticals and biologics *in vitro* is critical when maximizing temporal and economic investments in the drug development pipeline (Chen 2017). Evaluation of these pharmacologics for dose response as well as for synergistic effects produced through multi-agent cocktails prior to testing in preclinical models, aids in streamlining this workflow by reducing the number of compounds assessed with valuable animal models and limiting unnecessary costs. To perform these comprehensive screens, however, necessitates HT techniques to probe each culture condition with sufficient experimental

and biological replicates. Common systems that require extensive human handling, physical space, and reagent volume per replicate are therefore incompatible with *in vitro* pharmaceutical studies. Methods that limit manipulation of discrete samples, minimize the space required for culture, and reduce materials required for testing, are fundamental in enabling HT drug screens. In addition to sustaining compound screens, HT culture is also crucial in probing mechanisms involved in rare cellular events, such as cell fusion, genetic mutations, and cancer dormancy, while also enabling studies at the single cell scale to parse out population heterogeneities.

Whereas with the recent advances in polymer chemistry and biomaterials, it is possible to culture cancer cells in semi-physiologic substrates that more closely mimics native tumor environmental niches, such as collagen and Matrigel®. This method is thought to recapitulate the TME more accurately and permit detailed study of the interactions with the extracellular matrix, cell-cell crosstalk, signaling, and potential resistance to chemotherapy. Therefore, improved development of 3D platforms is vital for the continued scientific advancement, including but not limited to, the realm of cancer biology. To help fill this need, we present a microfluidic-based 3D collagen droplet platform (now called microtissues) capable of producing thousands of replicates an hour, while housing sensitive cells in favorable 3D microenvironments, and with an accompanying pipeline for screening and downstream analysis.

Section 1.2 – 3D Cell Culture Platforms

Encapsulation of cells within a hydrogel matrix is a long-standing approach to 3D culture that provides a physiologically relevant microenvironment for investigating cell behavior. Such methods are highly appealing for applications in the tissue engineering and regenerative medicine fields, but their use as enhanced disease models is indisputable. These systems are biologically advantageous compared to 2D systems as they can enable integrin binding to ECM binding motifs, provide appropriate biomechanical properties, and facilitate tissue level functional studies.

The conventional method to produce gels consists of depositing an aqueous hydrogel solution into standard tissue culture well-plates or dishes and subsequently polymerizing the solution with chemical, UV, or thermal crosslinking (Bell 1976). While compatible with diverse cell types and materials, the experimental power of this technique is restricted by the large volumes of cells and polymer required for casting, greatly limiting the number of experimental conditions and replicates that can be tested and preventing studies on highly precious cell sources (Joshi 2020). These restrictions ultimately reduce their use in academic labs investigating the role of pre-identified pathways linked to specific disease mechanisms (Srinivasan 2012) and for producing bulk tissue-level grafts for regenerative medicine (Slaughter 2009). Alternatively,

reliable, cost-effective, and rapid screening assays that remain amenable to 3D culture are in high demand prior to completion of expensive and time-consuming *in vivo* experiments. To address this need, current approaches use compartmentalized patterned gels in microarrays and droplet microspheres to miniaturize the gels while sustaining the 3D culture benefits.

Materials and Fabrication

During recent years, microgels have attracted great attention due to their unique incorporated microenvironment to study cell behavior. While microgel fabrication methods have been influenced by photolithography, microfluidics, and droplet technology, many current methods to produce cells subsequently encapsulated in microgels are fundamentally limited by their LT, poor scalability, and large size, ultimately creating a barrier for industry adoption. These large hydrogel tissues require extensive reagent and cell volumes, ultimately preventing heterogeneity studies involving precious cell sources or small cell numbers. However, recent advancements in the materials used for substrates and hydrogel solutions have improved the throughput and biological capabilities of this platform. Several models around this exist such as hydrogel microarrays, on-chip arrays, and dotted arrays. Therefore, an optimal model would maintain precise size control while allowing for scale-up and ensuring highly uniform physicochemical properties across the platform.

Droplets

Early methodologies for droplet microgels focused on fabricating a regenerative medicine platform and not a HTS one. Researchers dripped alginate solution from small gauge needles into a crosslinking chloride solution and produced thousands of alginate beads per hour (Focaroli 2016). These methods, though higher throughput than manually pipetting hydrogel solutions, produced large polydisperse beads at or approaching millimeters in diameter, despite attempts to reduce dispersity and decrease overall size with interdispersment of gas into the agarose solution (Peirone 1998). Further, the addition of an electric field reduced bead volumes and decreased bead diameter ultimately limiting size variability with additional protocols involving emulsification of aqueous hydrogel solution into pico-liter volume spheres followed by polymerization and resuspension in culture media (Chandrasekaran 2006). Despite improving length scales, these methods sustained the need for a minimally compatible crosslinking agent. Moreover, alginate and similar substances compatible with this protocol are inert with respect to mammalian cells are resistant to enzymatic degradation and cell spreading (Fang 2017).

Microfluidic-Based Droplets

Aqueous droplet microfluidics are invaluable due to their ability to perform complex biochemical reactions in series, as demonstrated by the prominently adopted droplet polymerase chain reaction (PCR), enzyme linked immunosorbent assays (ELISA), and single cell sequencing technologies (Macosko 2015). By leveraging microfluidic systems that reduce reagent volumes, static culture platforms amenable to automated HT liquid handling methods have been achieved. Multiple device designs have been developed that produce aqueous droplets and have proven equally adept at forming monodisperse, bioactive hydrogel microspheres, including T-junction, flow focusing, and acoustofluidics (De Lora 2020). Limitations, however, exist in material choices for encapsulation, where cytotoxicity of the oil phase and the viscosity of the hydrogel solution and the resulting shear forces must be considered (Ong 2008, Zhang 2009).

Developed out of the alginate microcapsules produced by multiphase and mixing, flow focusing devices enable on-chip polymerization (Ong 2008) and Janus particles fabrication (Zhang 2009). Others have utilized materials compatible with on-chip polymerization to encapsulate and culture cells in photo-crosslinked PEG microspheres, originally performed with bacteria, yeast, and prokaryotes (Cai 2014). Similar methodologies have subsequently been reported to encapsulate viable mammalian cells in synthetic, functionalized PEG matrices (Clausell-Tormos 2008**,** Brouzes 2012) and methacrylic gelatin (Joshi 2018). While enabling cell spreading, limited cell-ECM interactions and cell-cell interactions can be probed with these synthetic or bioinert materials as they prevent complete remodeling by the cells despite functionalization with cell-binding motifs. In addition, using the described droplet platforms has enabled fabrication of bioactive, ECM-based droplets using collagen (Jang 2016, Brett & Crampton 2016, Crampton & Cummins 2019, Cummins 2021), Matrigel® (Dolega 2015), and even decellularized matrices from various organs (Lee 2019).

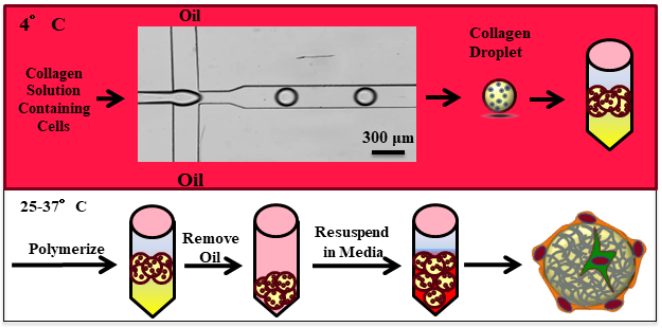

Fig. 1) Schematic of the microtissue platform adapted from (Crampton & Cummins 2018, 2019, Cummins 2021). Cell-laden microtissues are fabricated in a flow focusing microfluidic device and then polymerized. They are then resuspended in cell culture media the oil is removed and are ready for downstream experimentation. (Crampton & Cummins 2018, 2019, Cummins 2021).

Long-term culturing platforms coupling microwell platforms with ECM-based droplets have demonstrated the ability to culture constructs for up to two weeks while also demonstrating compatibility with a range of cell types. Due to the small volumes of reagents required by microfluidics, novel ECM-based microtissue platforms allow for efficient use of patient samples while minimizing waste and future studies should focus resources on validating their technology across numerous cell lines.

Readouts

Substantial developments have taken place in fabricating microgels which are readily compatible with a variety of materials, assays, and integrated biosensors. Hydrogel microarrays on slides have been combined with complimentary microarrays in which discrete combinations of compounds are used to enable complex culturing conditions for each gel within the array. Microarrays have proven highly useful in identifying variables that influence certain diseases such as nanoparticle embedded hydrogel for hyaluronidase (HAase) detection (Li 2017), and for their ability to be a stimulus-responsive fluorescent scaffold (Yang 2019). Recently through the Metachip system, Cho et al., demonstrated toxicology and dose response of 27 compounds combined with 3 enzyme isoforms on hepatoma cells encapsulated in alginate gels resulting in nearly a thousand conditions with replicates in a single experiment (Cho 2005). Microspherical systems have alternatively been utilized to perform HT permeability assays (Crampton 2018), to perform co-culture studies and improve tumor mimics (Hwang 2021), and to demonstrate tissue level functions of tissue-remodeling (Crampton & Cummins 2019, Cummins 2021). Future innovations in microgel readouts may provide insight into the mechanisms behind cell sprouting, and incorporation into medical field devices such as glucose monitors and MRI machines.

Outlook

To support the increasing translational usage of cells, a growing need for quality HT cell encapsulation technologies need continuous exploration. Unfortunately, many conventional devices encounter challenges including clogging, leaking, material swelling, high cost, and limited scalability. Strategies for fabricating a true HT microgel device continue to be analyzed including microfluidics (Kim 2019**,** Mohamed 2019), double emulsion **(**Krüger 2019), friction based **(**Enck 2020), emulsifying porogens (Xu 2019), and crosslinker-free techniques. However, while these platforms show promise, the large size of the gels, imaging concerns, and

accessibility remain significant concerns that are currently blocking broad microgel integration.

Respectively, microtissues are a promising candidate and hold great biopharmaceutical potential due to their high production rates, controllable microenvironments, and minimal use of valuable resources. The HT production of cells and readouts via the microtissue platform is currently siloed in cell specific applications and will need to continually evolve to a more universal platform through increased imaging capabilities and validation studies. Therefore, we present a microtissue platform capable of producing thousands of replicates and hour, while housing sensitive MPNST cells in favorable 3D microenvironments, with an accompanying pipeline for screening and downstream analysis.

CHAPTER 2

Microtissue Platform as a Model System for MPNST Screening

Section 2.1 – Introduction

The goal of this specific project is to advance a 3D collagen droplet microfluidic platform and to apply it as a model for culturing *ex vivo* PDX MPNST. The criteria for a robust, biologically relevant model in this context consist of the ability to: (i) control the cellular microenvironment, (ii) harbor viable cells in favorable culture conditions long term (~1 week), (iii) perform reproducible drug screening assays with multiple agents, and (iv) validation across numerous cell lineages. In addition to this criterion, any unique innovations, or modifications to the platform addressing challenges around deployment and scalability will be presented. The proceeding text is from a paper recently submitted for review by Bhatia H, Larsson A, Calizo A., et al. (2022).

Section 2.2 – *Ex vivo* to *in vivo* model of MPNST for precision oncology

Importance of the study

Genomic heterogeneity is a unique characteristic of MPNST that make them difficult to treat in the clinic. A preclinical model is needed that replicates the heterogenous nature of parental tumors and can be used to test candidate drugs. We successfully established 13 PDX and identified common somatic variants and chromosomal aneuploidy events. The PDX were further assembled into 3D microtissues, categorized as “robust”, “good”, or “unusable” on the basis of viable cell count. Treatment of "robust” and “good” microtissues with select drugs (trabectedin, mirdametinib, and olaparib) identified mirdametinib as an effective single agent. We also observed synergy upon combination drug therapy. Treatment of corresponding PDX with the same drugs showed similar response pattern as the 3D microtissues. We report the development of a novel *ex vivo* 3D microtissue platform that replicates *in vivo* PDX drug response.

Section 2.2.1 Introduction

Malignant peripheral nerve sheath tumors (MPNST) are aggressive soft tissue sarcomas with limited treatment strategies[1,2]. *NF1* gene inactivation and loss of neurofibromin (NF1) protein expression characterize the majority of NF1-MPNST [3]. *NF1* loss is necessary for MPNST development, but not sufficient for malignant transformation [4,5]. The cooperating genetic alterations found in MPNST include loss-of-function (LOF) alterations in *TP53*, *CDKN2A,* and polycomb repressor complex 2 (PRC2) genes (*EED/SUZ12*) [6–9], as well as Chr8 gain and other copy number changes [10–13]. A major barrier to improving outcomes is the absence of preclinical

models that accurately represent the heterogeneity found in MPNST. We have therefore generated the largest set of genomically characterized NF1-MPNST patient derived xenografts (PDX), and we have shown that these lines recapitulate the spectrum of genomic alterations that are seen in NF1-MPNST [10]. Our work is guided by strong scientific evidence that PDX provide a genomically-authentic and more patient-relevant model for pre-clinical drug evaluation than cell lines [14].

Human disease biology is profoundly complex and certain biological processes cannot be reproduced on plastic. Additionally, 2-dimensional (2D) cell cultures are prone to genetic drift and monolayer cultures are not representative of human disease [15–17]. Three-dimensional (3D) cultures bridge this gap between human cells and animal models [18]. These medium-throughput cultures mimic *in vivo* intercellular interactions and permit study of complex tissue structures. 3D cultures are potentially more predictive of clinical drug response than 2D cultures [19], and have been used extensively for cancer drug screening studies, but limited studies exist for NF1-MPNST [20(p),21,22]. We therefore cultured MPNST PDX cells *ex vivo* in engineered 3D microenvironments in order to recapitulate critical cell-cell and cell-matrix interactions that influence drug responses in human tumors.

We now report the successful development of a novel 3D collagen/Matrigel® microenvironment (hereafter referred to as microtissue) platform to assess drug response in MPNST. The cells in our microtissue model grow in association with a dense extracellular matrix (ECM), more akin to developing tumor rather than monolayer cell culture. Our comparison of microtissue drug response and PDX tumor drug response revealed significant similarities between the two model systems. Taken together, this *ex vivo* PDX-microtissue to *in vivo* PDX platform offers an ideal model system for drug discovery, drug response validation, and exploration of MPNST biology in a genomically heterogeneous system representative of the human condition.

Section 2.2.2 Materials and Methods

Study approval

Specimens were collected under IRB-approved protocols at Johns Hopkins University (protocol J1649) [23], Washington University at St. Louis (protocol 201203042), and University of Minnesota (protocol STUDY00004719). Patient subjects provided written informed consent prior to participation.

Human subjects and PDX tumor model establishment

Tumor pieces were collected following surgical removal, transported in DMEM

containing 10% FBS to the laboratory, and were used for implantation into mice. Tumor tissue was implanted dorsally into 5- to 6-week-old NOD-*Rag1*^{null} *IL2rg*^{null} (NRG) mice. When tumors were ~2cm x 2cm (or the mouse met other parameters that required its sacrifice), tumors were removed, minced, and engrafted into additional mice. This process was repeated for six passages. Engraftment success was defined as the ability of the PDX to be serially transplanted for six passages. JH-2-055-b represents the same line previously published as JH-2-055, but multiple samples have been processed from a single patient, and therefore JH-2-055-b has been renamed accordingly [24].

WES, WGS, and RNA-seq library preparation and sequencing

Normal germline, tumor, and xenograft samples from five patients (total 15 samples) were used for DNA sequencing. DNA libraries were constructed using KAPA HyperPrep Kits for NGS DNA Library Prep. For whole exome sequencing, exomes were captured by IDT exome reagentxGen Exome Research Panel V1.0; exome libraries were sequenced by NovaSeq6000 S4 300XP with ~200× coverage for normal samples and 800-1000x coverage for tumor/xenograft samples. For WGS, libraries were sequenced by NovaSeq6000 S4 300XP with 15-20x coverage. For RNA-seq, tumor and xenograft samples were used from five patients. Samples were prepared using TrueSeq stranded total RNA library kit with Ribo-Zero for rRNA depletion. Libraries were sequenced by NovaSeq6000 S4 300XP with targeted coverage of 30M reads per sample.

WES data analysis

WES data from eight patients reported previously [10] were used. WES sequencing FASTQ files were trimmed using Trimmomatic v 0.39 [25] and aligned against reference sequence hg38 via BWA-MEM [26]. Duplicate reads were marked using picard "Markduplicates". GATK V4.2 base quality score recalibration (BQSR) was used to process BAM files. For PDX sequence data, Xenosplit was used to filter mouse-derived reads using mouse (GRCm38) and human (hg38) reference genomes. Somatic single nucleotide variants (SNVs) and small insertions or deletions (indels) were detected using VarScan2, Strelka2, MuTect2, and Pindel, as previously described [10]. Variant filtering and annotation were done using Variant Effect Predictor (VEP) [27]. Common variants found in the 1000 Genomes MAF and GnomAD MAF > 0.05 were filtered out. Somatic variant plots were created with maftools v2.10.0 [28].

Copy number variant (CNV) analysis using WGS data

WGS data from eight patients reported previously [10] were used. Alignment of sequence

reads, removal of duplicate reads, and BQSR steps are as described above. CNVkit V2.0 was used to infer and visualize copy number. Normal pooled reference was first built from all normal samples. The reference was used to extract copy number information from tumor/xenograft sample BAM files. Heatmap was drawn using CNVkit's heatmap function.

Bulk RNA-seq analysis

Initial primary tumors and PDX samples were aligned to GRCh37. Mouse-derived reads were filtered using Xenosplit. RNA reads were quantified using the Salmon algorithm [29]. Gene counts and transcript counts were normalized by using the DESeq2 package [30(p2)].

PDX Cell Dissociation for 3D microtissue assembly

All mouse experiments were approved by the Institutional Animal Care and Use Committee (IACUC) at University of Minnesota under protocol #2101-38758A. For each PDX, a sample was minced in a basement membrane matrix and passed through a 1mL syringe (18-gauge needle) and injected into the flank of NRG mice (Jackson Labs). Once the xenograft tumors reached the maximum size allowed (2000mm^3), mice were euthanized, tumors were extracted in a laminar flow hood under sterile conditions, and were immediately digested using the human Tumor Dissociation Kit (130-095-929, Miltenyi Biotec) in combination with the GentleMACS Octo Dissociator (Miltenyi Biotec). The digested PDX was filtered through a 70μm cell strainer and then depleted of residual red blood cells using 1X RBC Lysis Buffer (eBioscience). Dead cells were removed from the digested PDX using a Dead Cell Removal Kit (130-090-101, Miltenyi Biotec). Murine cells were removed from the dead cell depleted fraction using a Mouse Cell Depletion Kit (130-104-694, Miltenyi Biotec). Cell viability was determined using flow cytometry and 7-AAD Viability Staining Solution (Biolegend). Cell counts were ascertained using the Countess (Invitrogen).

2D Culture Details

PDX cells were maintained in Dulbecco's Modified Eagle Medium High Glucose (ThermoFisher), 10% Fetal Bovine Serum (Gibco), and 1% Penicillin-Streptomycin (Gibco). All cultures were maintained at 37°C, 5% CO_2, atmospheric O_2 and 95% humidity in tissue culture-treated 24-well plates (Corning).

Microwell and Microtissue Fabrication

Microwell plates were fabricated following previously established methods [31]. For the

assembly of collagen microtissues, previously established protocols were followed [31–33]. Briefly, high-concentration rat tail collagen I (Corning) was buffered with 10 × Dulbecco's phosphate-buffered saline (DPBS), neutralized to pH 7.4, supplemented with 10% Matrigel® (Corning), diluted to 6mg/mL concentration, and mixed with cells ($6x10^6$ cells/mL). At 4°C, the collagen solution was partitioned into droplets using a flow-focusing microfluidic device. Tissues were collected in a low-retention Eppendorf tube and polymerized for 30 min at 25°C. The oil phase was then removed and the collagen microtissues were resuspended in culture medium.

Drug Treatment (3D microtissues)

Inhibitors used in this study were: 1 mM mirdametinib (S1036, Selleckchem) and 1 mM olaparib (S1060, Selleckchem) dissolved in DMSO, and 0.5 μM trabectedin (clinical excess from Washington University pharmacy, manufacturer Johnson & Johnson) dissolved in water. Drug stocks were serially diluted for 8-point dose curves with 4-fold dilutions between each dose. Combinations of trabectedin with mirdametinib or olaparib were kept in a fixed 1:2000 ratio, respectively, for each dose, or with trabectedin at a constant concentration of 0.5 nM. PDX cell-laden microtissue cultures were treated with single and dual agents by addition of the diluted agent(s), in DMSO, to their relevant concentrations in the culture medium. The cell encapsulated microtissue solution was then added to the agent-media solution to obtain desired concentration. Control samples were treated with DMSO (Sigma-Aldrich) diluted in culture medium.

Cell Viability Assay

Microtissues containing encapsulated PDX cells were fabricated and cultured. To assess cell viability, constructs were washed thoroughly with DPBS (Corning) and then incubated in the dark at 21°C for 30 minutes with a staining solution of 5 μM DRAQ5 (Invitrogen) and 5 μM Calcein AM (ThermoFisher). A Zeiss Axio Observer was used to image z-positions at 50 μm intervals over a distance of 250 μm and images were further analyzed using Cellpose (Stringer et al, 2021) and ImageJ (NIH). For experimental wells, live cell over total cell count ratio was normalized to vehicle-only treated cells to produce percent cell viability. Data were analyzed with GraphPad Prism and dose-response curves generated using nonlinear regression Log(inhibitor) vs. response-variable slope model.

Drug Treatment (PDX)

Animal experiments were approved by the IACUC at Johns Hopkins under protocol #MO19M115 and at Washington University under protocol #20190118. Female NRG mice were

purchased from Jackson Laboratory. Single cell suspension of tumor cells ($3x10^6$ cells per mouse, trabectedin/ olaparib) or minced tumor fragments (trabectedin/ mirdametinib) were implanted subcutaneously in the flank of 6- to 8-week-old NRG mice. Drug treatment started when tumors reached approximately 50-100 mm^3 in volume and continued for three weeks (trabectedin/ olaparib) and 5-6 weeks (trabectedin/ mirdametinib). Mice were randomized at 3-5 animals per treatment group to achieve similar mean tumor volume between groups. Drug doses and modes of delivery used in this study were: trabectedin (clinical access from Washington University pharmacy, manufacturer Johnson & Johnson) at 0.15 mg/kg weekly via tail vein injection; mirdametinib (SpringWorks Therapeutics, formulated in 0.5% HPMC and 0.2% Tween 80) at 1.5 mg/kg via oral gavage daily; and olaparib (Selleckchem) at 100 mg/kg via oral gavage daily. Tumors were measured two to three times weekly with calipers and tumor volume was calculated using the formula $L \times W^2(\pi/6)$, where L is the longest diameter and W is the width. Animals were euthanized when tumors reached ~2 cm or mice reached other endpoints as defined by institutional animal protocols.

Section 2.2.3 – Results

PDX established from human MPNST represent full tumoral heterogeneity.

PDX serve as a useful preclinical model for cancer drug screening studies. We previously reported on eight MPNST PDX lines [10], established by engrafting minced tumor or single cell suspension into immunodeficient NSG mice followed by serial passage (**Fig 2A**). Here, we broaden our sample size by including five additional PDX-tumor pairs. MPNST PDX lines were established from biopsy-proven NF1-MPNST between 2014 and 2021 at three institutions: Washington University, Johns Hopkins University, and University of Minnesota. Clinical parameters from the thirteen patients are summarized (data not shown).

To determine the inter-tumoral heterogeneity across the 13 PDX-MPNST pairs, we performed deep whole exome sequencing to assess single nucleotide variants (**Fig 2C**) and whole genome sequencing to assess copy number alterations (**Fig 2D**). Consistent with previous studies, we observed common mutations associated with MPNST, including *SUZ12* (7 of 13 pairs), *TP53* (2 of 13 pairs), and *EED* (2 of 13 pairs) (**Fig 2C**). Some unique mutations were also observed, including *MUC12* (3 of 13 pairs), *AGAP3* (3 of 13 pairs), and *AGAP9* (5 of 13 pairs). MUC12 is a membrane glycoprotein reported to be a biomarker and metastasis promoter for colorectal cancer [34(p12)]; the AGAP family of proteins also promotes cancer cell invasiveness [35]. Mutations in the DNA repair gene *PBRM1* were observed in 1 of 13 pairs. Copy number analysis also revealed significant heterogeneity, and frequent gains in Chr8 (10 of 13 pairs; **Fig 2D**). Somatic variants in

some genes were found only in the PDX but not in the parental tumors; this finding can be attributed to expansion of select cell populations during PDX establishment, or sampling bias due to intra-tumoral heterogeneity. Consequently, certain variants are observed at a higher frequency in PDX than the parental tumors, suggestive of engraftment-related clonal selection within PDX, as observed previously [36].

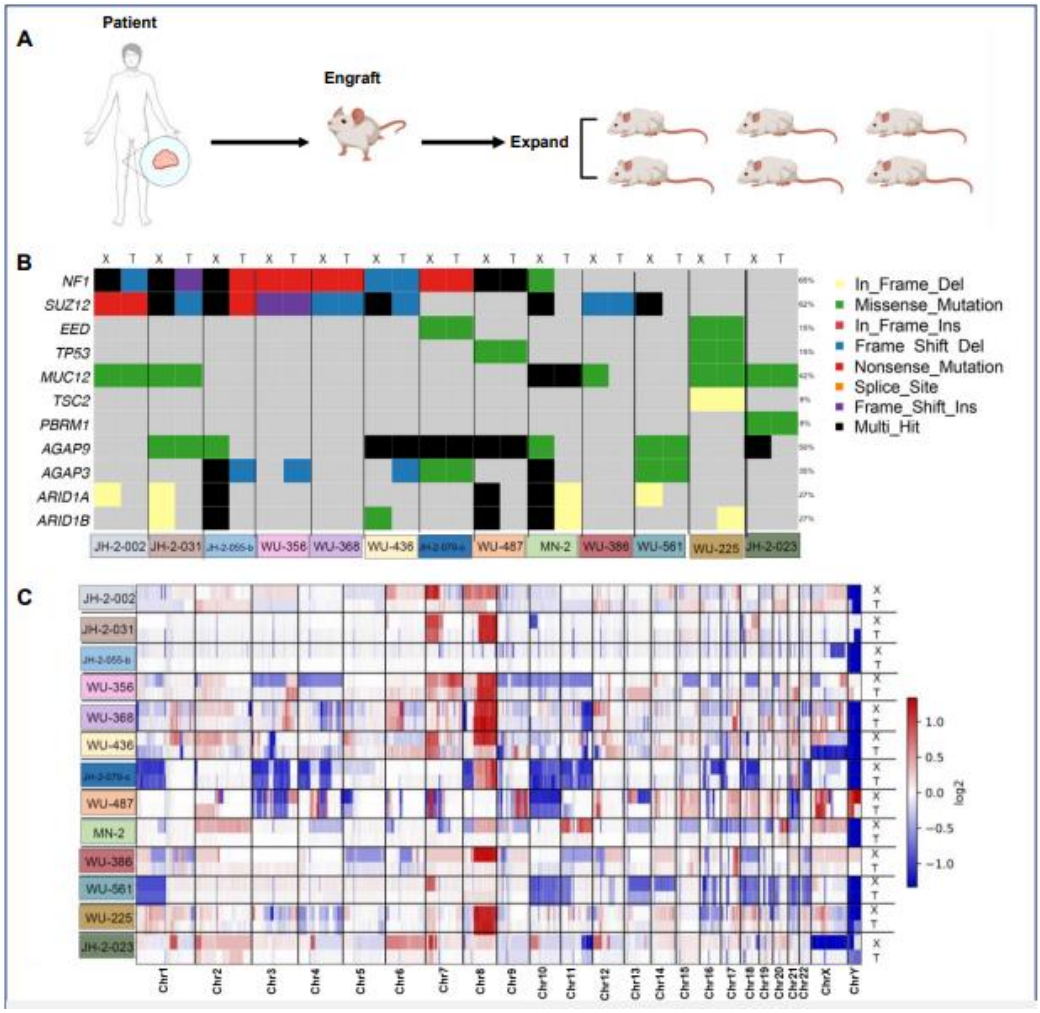

Figure 2. Diverse MPNST patient tumors used in separate models.
A.) Schematic description of patient derived xenografts engrafted into NRG mice for drug studies. B.) Heatmap of single nucleotide variants across all 13 PDX-tumor pairs (X = PDX; T = parental tumor). Each somatic variant is present in only a fraction of samples. Percent-wise distribution is shown on the right. C.) Copy number variations in 13 PDX-tumor pairs. (Bhatia H, Larsson A, Calizo A, et al. 2022 *Submitted)*

Dissociated PDX exhibit limited growth in two-dimensional culture and as spheroids.

PDX are a costly, time-consuming model for *in vivo* drug studies, prompting an interest in an alternative platform that maintains MPNST heterogeneity and is suitable for drug response studies. PDX were passaged in NRG mice, dissociated from mice, and cultured as two-

dimensional tissues on plastic. Six of thirteen PDX tested could be established as cell lines, and most PDX could not form spheroids in a collagen-free environment. After two days of growth in the collagen-free format, only MN-2 and JH-2-031 began to aggregate (**Fig 4A**). After seven days in culture, MN-2 exhibited a tight spheroid formation while JH-2-031 cells remained a loose aggregate (**Fig 4B**). The limited growth as spheroids suggest that this application is not a viable option for drug response studies. Further, neither of these two culture conditions reflect a developing tumor as they lack sufficient stroma and components of the ECM.

Three-dimensional engineered microenvironments, or 3D microtissues, are successfully created from dissociated PDX.

We therefore attempted to create three-dimensional (3D) microtissues, based on prior experiences with other cell types [32(p)]. Dissociated PDX were depleted of mouse and dead cells and assembled into 3D microtissues with the addition of collagen and Matrigel® for tissue support (**Fig 2A)**. In the 3D microtissue format, some PDX failed to proliferate or grew only for a few days, and thus, were removed from drug studies (data not shown). We also observed that several PDX remodeled the collagen matrix. Within two days in microtissue culture, MN-2 began to compact its collagen fibers (data not shown). After seven days, MN-2 completely remodeled its microenvironment, forming small round masses of cells and collagen. Other PDX took longer to remodel their microenvironment (11 days for JH-2-079-c) or not at all (WU-225; data not shown). Differences in collagen compaction rates have been observed previously [31].

Given this variability, microtissues were ranked for quality based on the initial percent cell viability and the difference between percent cell viability at 48 hours after assembly and just prior to assembly. We qualified them as robust (>90% viability), good (>50%), or unusable (<50%) and only used those categorized as robust or good for drug studies. Four out of nine PDX-microtissues tested met these criteria: MN-2, JH-2-002, JH-2-079-c and WU-225 (data not shown), representing the successful development of a 3D microtissue platform generated from PDX (**Fig 2B**).

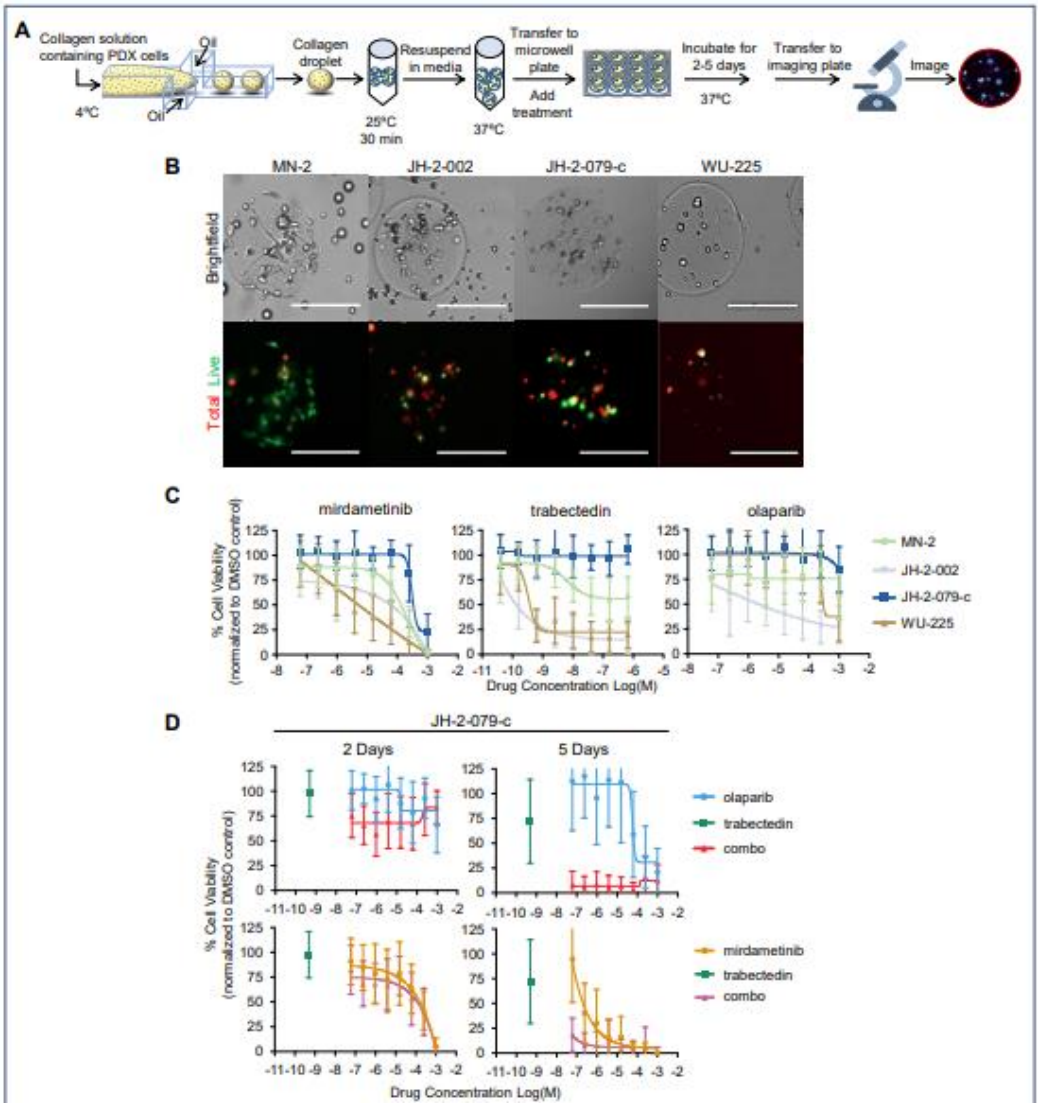

Figure 3. PDX 3D microtissues are inhibited with trabectedin drug combinations. A.) Schematic description of dissociated patient derived xenograft tumors processed into 3D microtissues. B.) Representative brightfield and fluorescent images of PDX 3D microtissues made from MN-2, JH-2-002, JH-2-079-c and WU-225, stained with calcein AM (live) and DRAQ5 (total) after two days in culture. Scale bars: 200µm. C.) Dose response curves of four PDX 3D microtissues exposed to single agents mirdametinib, trabectedin or olaparib for two days in culture. Data points and error bars represent mean ± SD, n ≥ 10. D.) Dose response curves of JH-2-079-c exposed to trabectedin combinations with either mirdametinib or olaparib for two or five days in 3D microtissues. Trabectedin concentration was kept constant (0.5 µM) with varied concentrations of mirdmetinib or olaparib. Data points and error bars represent mean ± SD, n ≥ 10. (Bhatia H, Larsson A, Calizo A, et al. 2022 *Submitted)*

Initial microtissue drug studies demonstrate selective response to single agents and combination therapies.

In order to test the drug-screening capability of this novel platform, we chose three drugs

predicted to generate a response, as proof-of-principle. Mutations in DNA repair genes are found in up to 25% of MPNST [10,37] (**Fig 2C**), leading to selection of olaparib, a PARP inhibitor. We selected trabectedin as a chemotherapeutic that could be combined with a PARP inhibitor or other targeted therapies. Trabectedin distorts the structure of DNA and interferes with the nucleotide excision repair (NER) system [38], potentially leading to synthetic lethality in combination with a PARP inhibitor. Finally, we chose mirdametinib (PD0325901) as a representative MEK inhibitor, as *NF1* loss results in hyperactive RAS-RAF-MEK-ERK signaling and MEK inhibition is partially active in NF1-deficient tumor cells [39,40].

Since PDX-derived 3D microtissues are more reflective of human disease than 2D or spheroid culture, we hypothesized that drug response studies in microtissues would inform *in vivo* activity. We initially tested trabectedin plus mirdametinib and trabectedin plus olaparib in fixed ratios of 1:2000. We tested each drug with an 8-point dose range with 4-fold dilutions between doses. Mirdametinib had the strongest effect on cell viability for each of the four microtissues, while olaparib and trabectedin had varied effects (**Fig 3C**). JH-2-079-c responded the least to all three drugs; it is also the only PDX derived from recurrent tumor and therefore may be intrinsically more drug-resistant. WU-225 was the most responsive to trabectedin and mirdametinib (**Fig 3C**). While both WU-225 and JH-2-079-c have mutations in components of the PRC2 complex, WU-225 has additional mutations in *TP53* (**Fig 2B**).

Low concentration of trabectedin and longer exposure time enhances cytotoxicity in 3D microtissue combination studies.

These fixed-ratio drug combinations did not exert an enhanced effect over single agents in any of the microtissues (data not shown). We hypothesized that synergistic or additive effects in the fixed-ratio regimen were underestimated due to both the short time course and the robust response to high single doses of trabectedin. Therefore, we chose a low dose of trabectedin (0.5 nM) to combine with each of the eight doses of either olaparib or mirdametinib. An enhanced effect emerged in both combinations but was more pronounced with olaparib plus trabectedin (**Fig 3D**). Additionally, JH-2-079-c exhibited a dramatic reduction in cell viability after five days in culture, even at the lowest concentrations of olaparib or mirdametinib (**Fig 3D**). These data show that drug synergy can be observed in NF1-MPNST PDX cells cultured for longer than two days in 3D.

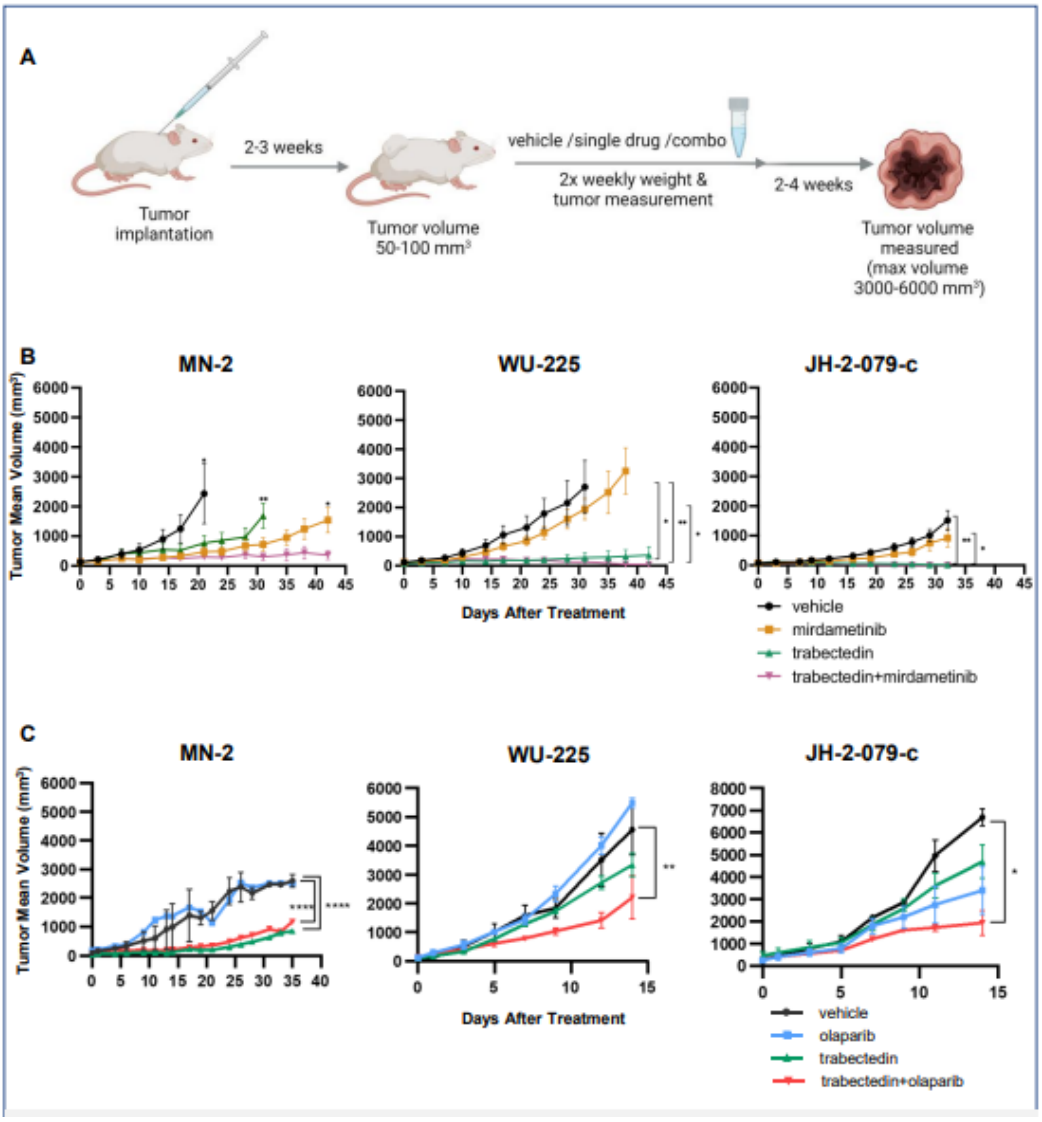

Figure 4. *In vivo* tumor growth is inhibited with trabectedin treatments.
A.) Schema describing timeline of drug administration following PDX engraftment. B.) Tumor volume response to mirdametinib, trabectedin or their combination in MN-2, WU-225, and JH-2-079-c PDX grown in mice. C.) Tumor volume response to olaparib, trabectedin or their combination in MN-2, WU-225, and JH-2-079-c PDX grown in mice. Data points and error bars represent mean ± SEM n=3-5, ANOVA was used to assess statistical significance (****P < 0.0001; ***P < 0.001; **P < 0.01; *P < 0.05). (Bhatia H, Larsson A, Calizo A, et al. 2022 *Submitted)*

Trabectedin treatment inhibits in vivo tumor growth in MPNST PDX, consistent with the microtissue model.

We sought to validate our findings from microtissues in *in vivo* PDX models. Tumor-bearing NRG mice were treated with either single agent or combination drugs (**Fig 4A)**. MN-2 showed modest sensitivity to trabectedin and a more potent effect from the trabectedin and

mirdametinib combination (**Fig 4B**). These drugs had similar single agent responses in the microtissues. In contrast, WU-225 demonstrated enhanced tumor growth inhibition to single agent trabectedin (**Fig 4B**). The combinations of trabectedin and mirdametinib or trabectedin and olaparib resulted in dramatic inhibition of tumor growth in WU-225 (**Fig 4B, C**). JH-2-079-c had limited response to single agents *in vivo*, similar to observations *ex vivo*. However, combination therapy with trabectedin and olaparib (**Fig 4C**, $p=0.0164$) and trabectedin and mirdametinib (**Fig 4B**, $P < 0.05$) did significantly reduce tumor volume *in vivo*, similar to five-day *ex vivo* studies. In contrast, MN-2 demonstrated enhanced sensitivity to trabectedin alone ($P < 0.0001$) as well as mirdametinib single agent ($P < 0.05$). However, no increase in effectiveness was observed with trabectedin and olaparib combination therapy, while a significant benefit was observed with the combination of trabectedin and mirdametinib versus trabectedin treatment alone (**Fig 4B, C**). These data together confirm that the findings from the 3D microtissue model are predictive of *in vivo* response.

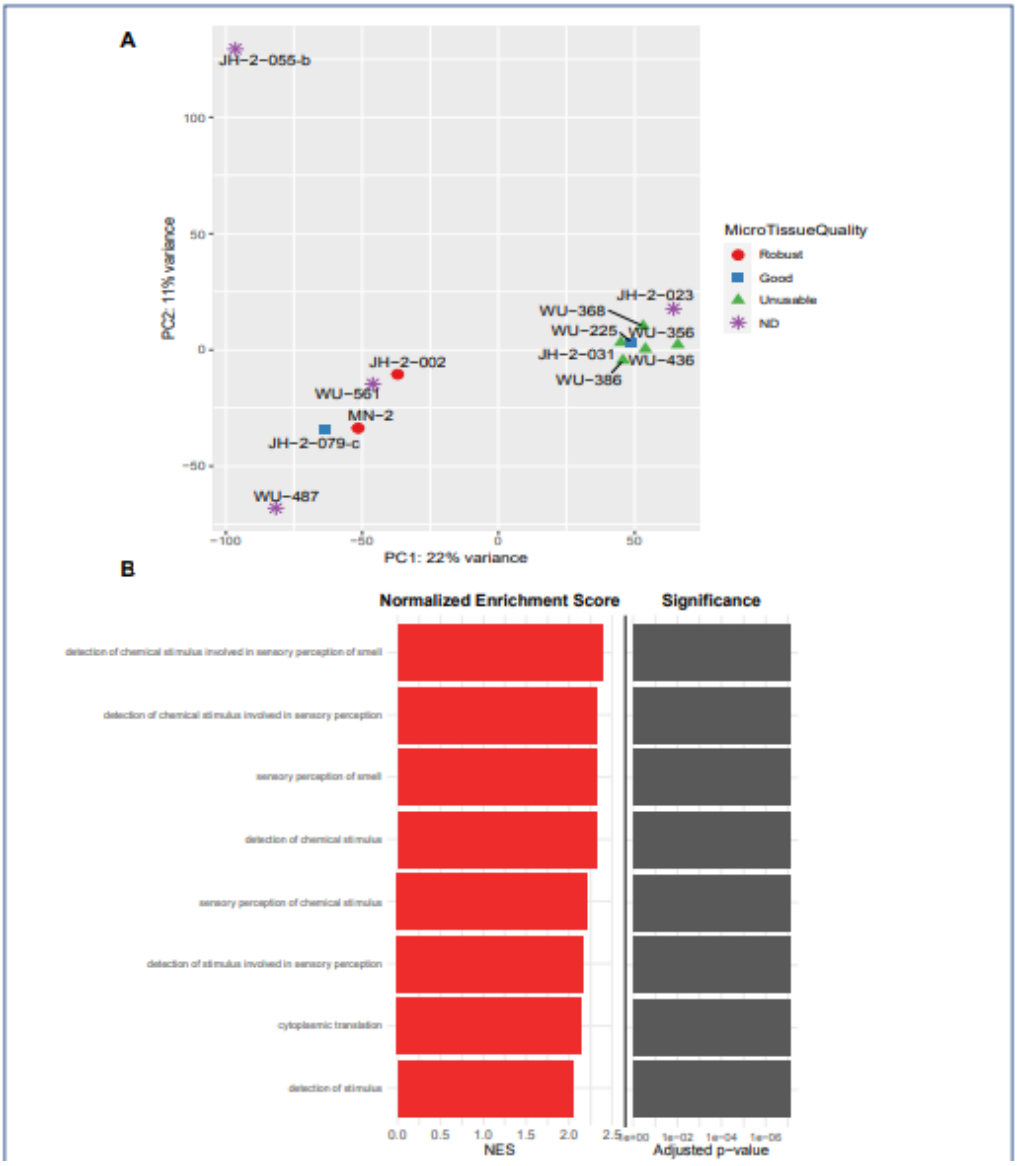

Figure 5. Gene expression analysis of microtissues by their quality.
A.) Two-dimensional embedding of gene expression of each patient sample. Shape indicates microtissue quality from Table 1. B.) Biological processes enriched in microtissues that exhibit robust or good growth compared to those that do not grow in culture. Adjusted p-value < 0.01. (Bhatia H, Larsson A, Calizo A, et al. 2022 *Submitted)*

Gene expression analysis of PDX samples identifies key pathways that may predict the quality of an assembled microtissue.

Given the genetic diversity of the PDX samples as well as the differences in growth patterns within the microtissues, we evaluated gene expression signatures by RNA-sequencing (**Fig 5A)**. Using principal components analysis (PCA), we observed that the first principal component, depicted on the x-axis, segregates samples that grow well in the microtissues (left)

from those that do not (right). This clustering pattern suggests that we can predict the growth characteristics of microtissues on the basis of gene expression data.

We attempted to identify whether specific biological pathways were differentially represented between the two sets of samples. We found that 525 genes were differentially expressed (adjusted $p < 0.01$) (data not shown). Gene enrichment analysis identified pathways related to perception of external (chemical) stimuli to be enriched in "robust" and "good" microtissues (**Fig 5B**), which is correlated with their enhanced ability to respond to signals in their extracellular environment [41].

Section 2.3 Discussion

Mutational heterogeneity and DNA aneuploidy commonly seen in MPNST present challenges to the successful development of effective therapies. Many pre-clinical platforms rely on genetically engineered mouse models, which are not capable of representing the full heterogeneity of genomic alterations that exist in patient tumors, limiting the ability to translate to the clinic. To address this problem, we have developed a PDX-based *ex vivo* 3D microtissue platform. The entire system offers several advantages, including the ability to perform rapid and cost-effective drug response studies, the capacity to validate drug effectiveness, and the potential to optimize the tumor microenvironment as desired.

The PDX tumor models successfully reflect the genomic diversity of MPNST and accurately recapitulate the genetic signature of corresponding parental tumors. We identified common genetic alterations in the 13 PDX-MPNST pairs, including somatic *NF1* mutations in 8 of 13 pairs. Five cases, WU-386, WU-561, WU-225, MN-2, and JH-2-023, were presumed to have a second hit in *NF1* through another mechanism. The occurrence of NF1 cases without an identifiable second hit in *NF1* has been established [42]; these cases presumably have mutation(s) in non-coding region(s) or copy number loss of *NF1*. We also observed mutations in both *NF1* and *SUZ12* or *EED* in 7 of 13 PDX-MPNST pairs, and *TP53* in 2 of 13 pairs. These PDX are overall representative of the parental tumors, although some extent of clonal evolution was observed in PDX WU-386, JH-2-055-b, and JH-2-002, where mutations not seen in the parental tumor were observed in the PDX. This finding is consistent with other studies in which clonal complexity of parental leukemia may be altered in corresponding PDX [43].

While the *in vivo* PDX model has strong advantages for drug efficacy studies, these experiments can be time-intensive and costly. In the last decade, engineered 3D microenvironments have garnered considerable attention as an alternative preclinical model, as small formations that closely mimic the natural tumor microenvironment without the complexity

and cost of maintaining animal colonies needed for *in vivo* studies [44]. As sensitivity of cancer cells to drug treatment is strongly influenced by the tumor stroma [45], the 3D microtissues developed from PDX lines are an ideal platform to study drug response. The collagen matrix used in microtissues, which is absent in traditional 2D culture, favors cell-cell interactions by mimicking the ECM [32,33]. Additionally, we found that dissociated PDX tumor cells could rarely grow as tight spheroids, limiting the utility of this 3D model.

Utilization of this system has already informed the potential activity of several therapeutic agents. Assessment of cell viability following treatment with selected drugs identified mirdametinib as a potent agent against all microtissues tested. The combinations of trabectedin and mirdametinib or trabectedin and olaparib also demonstrated anti-tumor activity *ex vivo* and *in vivo*, suggesting that these are potential combinations to test in clinical trials.

Finally, the 3D microtissue system can be modified to systematically test, in isolation, factors that enhance drug response. For example, differential response of patient-matched organoids to chemotherapeutic agents against PDAC (pancreatic ductal adenocarcinoma) have been reported. [46] Addition or removal of paracrine factors from organoid growth media modulated drug response patterns in these models. It is possible, therefore, that the microtissue model may also be enhanced by the addition of cytokines, ECM components, stromal cells, and/or conditioned growth media.

Drug response patterns observed in our microtissue model may be linked to differences in gene expression, in accordance with prior studies.[46] We observed homologous transcriptional clustering across microtissues that were categorized as either “robust” or “good” versus “unusable”. Pathway enrichment analysis identified genes related to perception of external stimuli, which may be linked to the ability of these lines to grow well. Cancer cells grown in 3D cultures are more receptive to environmental stimuli from all directions that properly represents the *in vivo* stimuli pattern [41] . Hence, enhanced receptiveness to environmental stimuli might be crucial for the development of viable 3D microtissues.

The notable limitations of our PDX-to-microtissue model are the low success rate of establishing “robust” or “good” microtissues, and limited growth duration of established microtissues. We expect that modification of growth media components will enhance the durability of our novel platform. Efforts are underway to improve growth conditions that permit the establishment of additional 3D microtissues that can grow for longer periods of time.

In summary, we report the development of a novel medium- to high-throughput model system for testing candidate drugs in MPNST, using an *ex vivo* microtissue platform followed by PDX testing for in vivo validation. Future studies will aim to test new drug combinations and to

elucidate components of the TME that effectively condition drug response.

Acknowledgements

The authors thank SpringWorks Therapeutics for supplying mirdametinib.

Statistics

Two-way ANOVA was used to calculate statistical significance. Analyses were considered statistically significant if $P < 0.05$.

Data availability

Data generated in this study have been deposited in the Sage Bionetworks NF Data Portal platform (https://www.synapse.org) with identification number syn21984813.

Authorship

Performed experiments and analyzed data: HB, ATL, AC, KP, XZ, EC, JFT, SO, KBW, ALC, TJ, DS. Analyzed sequencing data: KY, YL, JB, JCP. Wrote the manuscript: HB, ATL, AC, CAP, DAL, SJCG, DKW, ACH. Designed the study and acquired funding: SJCG, CAP, DAL, DKW, ACH.

Funding

This work was funded by grants from the NF Research Initiative (NFRI) and the St. Louis Men's Group Against Cancer (to ACH).

Conflict of interest

ACH: consultant for SpringWorks Therapeutics and AstraZeneca; grant funding from Tango Therapeutics. DAL: co-founder of and equity in NeoClone Biotechnology, Inc., Immusoft, Inc., and Luminary Therapeutics, Inc.; Senior Scientific Advisor and on the Board of Directors of Recombinetics, Inc.; research funding from Genentech, Inc. CAP: consulting for Genentech/Roche and Day One Therapeutics; research grant funding from Kura Oncology and Novartis Institute for Biomedical Research.

CHAPTER 3

Conclusions

Section 3.1 – Future Directions and Current Limitations

To this point, the concentration has been on a readily scalable, novel, 3D cell culture platform, with specific focus around microtissues. Alongside a firm understanding of the models presented and their limitations, future novel systems may provide important discoveries and advances in the pursuit of validating a truly accessible HTS 3D model. While there is currently excitement in the scientific community around novel HT models, we must step back and reassess the current state of the technology. Many current models are difficult to fabricate, LT, and do not accurately recapitulate *in vivo* physiology and pathophysiology. Additionally, there is still a lack of profound qualitative and quantitative evidence demonstrating such models have reproducible results and better predict clinical response relative to existing *in vivo* approaches (Scannell 2016, Carragher 2018). Ultimately, several critical challenges remain to be solved for these models including non-destructive real-time assays, robust imaging pipelines, and general validation across multiple unique cell lines.

By using current and future technologies, drug-to-outcome relationships could be identified earlier in the discovery pipeline, thereby reinforcing the need for a quality 3D model. Ever more sophisticated novel imaging analysis tools across 3D platforms continue to be produced and are contributing to highly dynamic and quantitative read-outs of target biology **(**Li 2017, Wang 2019, German 2021). Along with imaging, robust assays that more closely resemble true *in vivo* tissue level function are becoming increasingly important. Due to many technologies requiring vast amounts of resources to accomplish HT, a device capable of accomplishing similar results with reduced resources will be crucial. With cell sourcing being a large source of variability, harmonizing quality control standards for sourcing cells, storage, stability, and cGMP-compliance are crucial aspects in validating culture models (Rashid 2010). To address these concerns, a recent study produced cGMP-derived constructs amenable to 3D culture and employed a robust validation process laying groundwork for all novel HT models attempting validation (Seng 2018). Furthermore, a SWOT analysis pipeline for high-content analysis of 3D cellular systems has been created and clearly highlights the need to harmonize quantification and data-analysis standards (Carragher 2018).

Additionally, collaborative partnerships between industry and multidisciplinary academic researchers need to be continually formed focusing on enabling quality 3D models and discussing the value of these methods to standardize guidelines in the community; specifically, to highlight

the lack of robust validated 3D related methodologies, and readily deployable imaging software tools that enable robust quantitative and quantitative analysis.

Despite clear progress in the field with frequent technology occurring, several universal challenges persist, such as the inability to bulk synthesize information on critical subsets of cells, and therefore being forced to average information across an entire population (Das 2017, Boyer 2018, Shao 2019, Liao 2020, Utama 2020). Thus, there has been an increasing interest in technologies that enable true HT handling of cells individually and facilitate studies into cellular heterogeneity. Existing techniques, however, are often associated with high economic impact, limited throughput, work primarily on assays in isolation, and are generally completed in academic settings. If we reassess preclinical assays and necessary biological testing, it becomes apparent that easy recovery and downstream analysis is essential for technologies to progress (Carragher 2018).

Section 3.2 – Conclusion

The primary goal was to advance a microfluidic platform to be capable of housing *ex vivo* PDX MPSNTs, and to run single and combinatorial drug screens over time. It was found that several specific conditions such as ECM (collagen and Matrigel®), media, and a quality isolation are needed for optimal MPNST health *in vitro,* in terms of viability. In the presented microtissue model, a 6mg/mL collagen solution with 10% Matrigel® (v/v) was used to house the cells. Cell density qualitatively showed a positive response between density and viability, specifically, 6M cells/mL in this case (data not shown). However, preliminary studies may show an even higher cell density can be used with success (data not shown) and is of consideration for future work. Additionally, the media formulation was initially not found to be an obvious significant factor of the model; however, recent studies (**Fig. 6**) may show a higher relationship of media and cell health than previously believed.

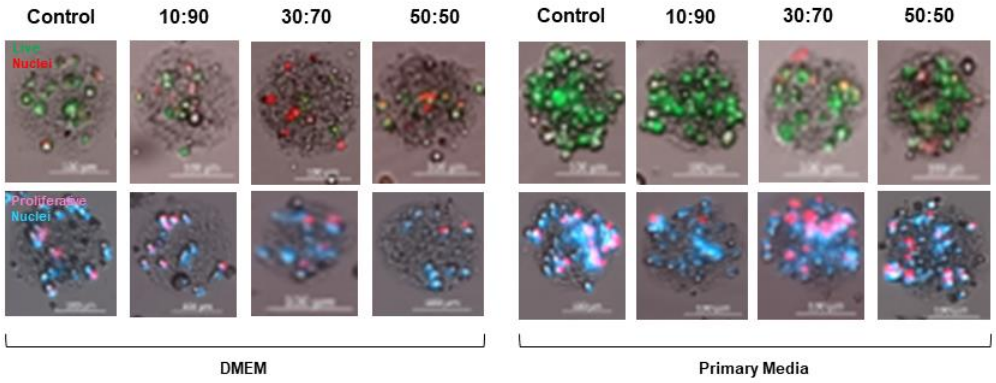

Fig. 6.) Qualitative depiction of representative MPNST sample in microtissues. Two

medias (DMEM and Primary Media) with various conditioned media: media ratios (50:50, 90:10, 70:30) and control were used. Scale bar (100um). (Conniff 2022)

Several vital modifications were made to the platform workflow to make it capable of running relatively large drug screens for the project. One modification was the incorporation of a cell strainer which helped diminish the amount of oil present in the culture (data not shown). This partial elimination of residual oil made downstream image analysis possible and sped up the fabrication process by reducing multiple waiting steps. Another modification was around the creation of a custom image analysis pipeline. The image analysis allowed us to consistently accumulate large amounts of viability data and was paramount to the success of this specific project. Fabricating a highly hydrophilic surface with polydopamine sped up the process of stamping microarrays from ~48hrs down to ~3 hours (**Fig. 7**). A re-design of aspirating devices allowed for the aspiration of liquids from common plate sizes and reduced the workload required when staining large sets of microtissues (**Fig 7. A**). Additionally, the creation of custom-made stamps increased the stamping throughput from 1 plate to 4 plates an hour, something vital for the success of this specific project (**Fig 7. B)**.

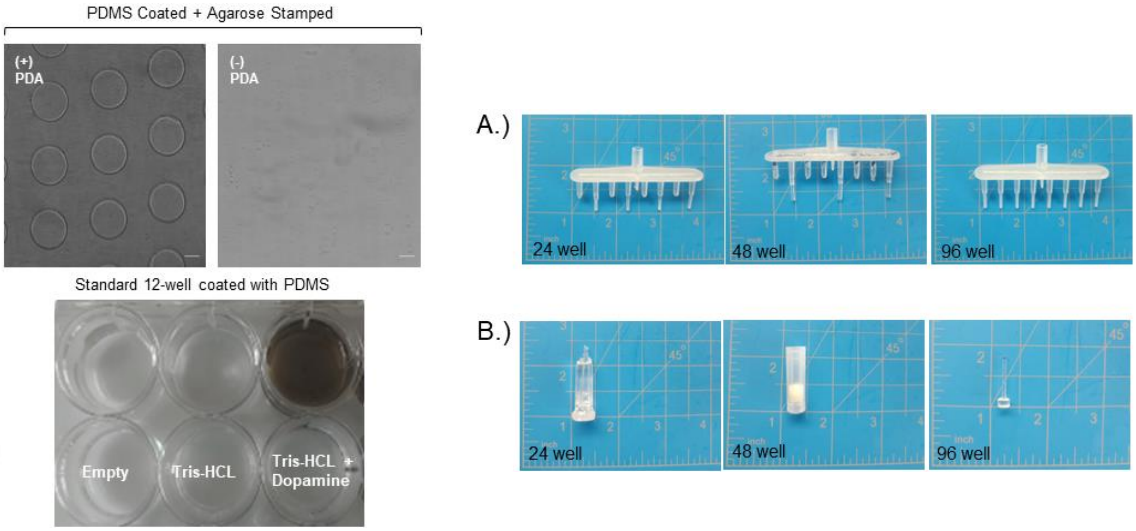

Fig. 7.) Polydopamine hydrophilic coating of a 12-well plate with accompanying microarrays stamped showing feasibility of method. A.) Shows multiple aspirating devices re-designed to fit various commonly used plates. B.) Shows multiple custom-made stamps for use in 24, 48, and 96-well plates and microwell array shapes and sizes (not pictured). (Conniff 2022)

The future image analysis pipeline quickly provides measurements on single cell resolution made possible through a laser scanning confocal microscope and semi-automated analysis script (data not shown)

With non-destructive real-time assays being rare in the field, we developed a novel method of relating glucose consumption to cell number to help address this gap in technology (**Fig. 8**).

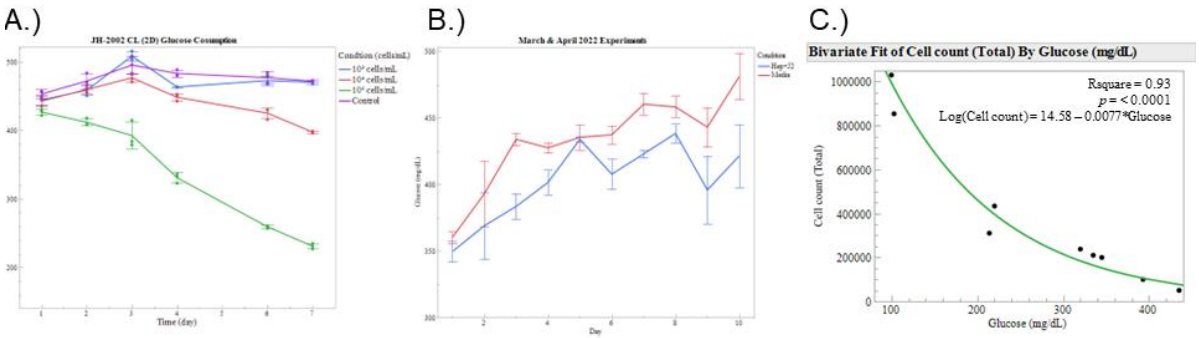

Fig. 8.) Fast, cheap, and effective method of glucose testing. A.) Shows a MPNST cell line tracking glucose consumption over time and its relation to starting cell number. B.) Shows multiple hepatocytes and 3T3-J2 fibroblast co-culture experiments and their relationship to media control tracked over 10 days. C.) Shows a correlation ($R^2 = 0.93$) of the number SW480 colorectal cancer cells in 2D and its relationship to glucose consumed over time. (Conniff 2022)

Current infrastructure and characterization around *ex vivo* PDX MPNST phenotypes and culture conditions remains an understudied space. Future understanding around the heterogeneity and uniqueness of each individual sample *in vitro* may help provide high quality preclinical research and thus improved individualized care downstream. Additionally, multiplexing molecular biology methods, such as RNA sequencing, with the current platform could provide insights into the potential similarities and differences between *in vivo,* 2D, and 3D models.

With microtissues being well-suited for easy adoption, microcarriers with a proven pipeline for industry implementation, and the resource saving potential of microfluidics, a complementary model compatible across multiple unique sensitive cell types has tremendous potential. As the technology in the field progresses, novel HT cell culture technology cannot just be convenience based; biologically relevant assays on primary cells/phenotypes, increased sensitivity, and highly reproducible tests are required. Thus, the next generation of 3D cell models are likely to be derived from the continued development of microtissue technology.

BIBLIOGRAPHY

Antoni, D., Burckel, H., Josset, E., & Noel, G. (2015). Three-Dimensional Cell Culture: A Breakthrough in Vivo. In International Journal of Molecular Sciences (Vol. 16, Issue 12, pp. 5517–5527). MDPI AG. https://doi.org/10.3390/ijms16035517

Baker, B. M., & Chen, C. S. (2012). Deconstructing the third dimension – how 3D culture microenvironments alter cellular cues. In Journal of Cell Science. The Company of Biologists. https://doi.org/10.1242/jcs.079509

Bednarek , Briana. (2021). Development of a Microvascular Network in a Microfluidic Model. Retrieved from the University of Minnesota Digital Conservancy, https://hdl.handle.net/11299/224899.

Bell RP (1973) The Proton in Chemistry. 2nd. ed., Chap. tl. Chapman and Hall, London

Bhatia H, Larsson A, Calizo A, Pollard K, Zhang-X, Conniff E, Tibbitts J, Osum S, Williams K, Crampton A, Jubenville T, Schefer D, Yang K, Lyu Y, Bade J, Pino J, Gosline S, Pratilas C, Largaespada D, Wood D, Hirbe A. (2022) Ex vivo to in vivo model of malignant peripheral nerve sheath tumors for precision oncology. *NeuroOncology*. Submitted.

[25] Bolger AM, Lohse M, Usadel B. Trimmomatic: a flexible trimmer for Illumina sequence data. Bioinformatics. 2014;30(15):2114-2120. doi:10.1093/bioinformatics/btu170

Boyer, C., Figueiredo, L., Pace, R., Lesoeur, J., Rouillon, T., Visage, C. L., Tassin, J.-F., Weiss, P., Guicheux, J., & Rethore, G. (2018). Laponite nanoparticle-associated silated hydroxypropylmethyl cellulose as an injectable reinforced interpenetrating network hydrogel for cartilage tissue engineering. In Acta Biomaterialia (Vol. 65, pp. 112–122). Elsevier BV. https://doi.org/10.1016/j.actbio.2017.11.027

[44] Brancato V, Gioiella F, Profeta M, et al. 3D tumor microtissues as an in vitro testing platform for microenvironmentally-triggered drug delivery systems. Acta Biomaterialia. 2017;57:47-58. doi:10.1016/j.actbio.2017.05.004

[45] Brancato V, Kundu B, Oliveira JM, Correlo VM, Reis RL, Kundu SC. Tumor-Stroma Interactions Alter the Sensitivity of Drug in Breast Cancer. Front Mater. 2020;7:116. doi:10.3389/fmats.2020.00116

[33] Brett ME, Crampton AL, Wood DK. Rapid generation of collagen-based microtissues to study cell–matrix interactions. Technology. 2016;04(02):80-87. doi:10.1142/S2339547816400094

Brouzes, E. (2012). Droplet Microfluidics for Single-Cell Analysis. In: Lindström, S., Andersson-Svahn, H. (eds) Single-Cell Analysis. Methods in Molecular Biology, vol 853. Humana Press. https://doi.org/10.1007/978-1-61779-567-1_10

Cai, H., Sharma, S., Liu, W., Mu, W., Liu, W., Zhang, X., & Deng, Y. (2014). Aerogel Microspheres from Natural Cellulose Nanofibrils and Their Application as Cell Culture Scaffold. In Biomacromolecules (Vol. 15, Issue 7, pp. 2540–2547).

American Chemical Society (ACS). https://doi.org/10.1021/bm5003976

Carragher, N., Piccinini, F., Tesei, A. *et al.* Concerns, challenges and promises of high-content analysis of 3D cellular models. *Nat Rev Drug Discov* 17, 606 (2018). https://doi.org/10.1038/nrd.2018.99

Chandrasekaran, A., Avci, H. X., Ochalek, A., Rösingh, L. N., Molnár, K., László, L., Bellák, T., Téglási, A., Pesti, K., Mike, A., Phanthong, P., Bíró, O., Hall, V., Kitiyanant, N., Krause, K.-H., Kobolák, J., & Dinnyés, A. (2017). Comparison of 2D and 3D neural induction methods for the generation of neural progenitor cells from human induced pluripotent stem cells. In Stem Cell Research (Vol. 25, pp. 139–151). Elsevier BV. https://doi.org/10.1016/j.scr.2017.10.010

Chen, C., Townsend, A. D., Sell, S. A., & Martin, R. S. (2017). Microchip-based 3D-cell culture using polymer nanofibers generated by solution blow spinning. In Analytical Methods (Vol. 9, Issue 22, pp. 3274–3283). Royal Society of Chemistry (RSC). https://doi.org/10.1039/c7ay00756f

Cho, S. H., Oh, S. H., & Lee, J. H. (2005). Fabrication and characterization of porous alginate/polyvinyl alcohol hybrid scaffolds for 3D cell culture. In Journal of Biomaterials Science, Polymer Edition (Vol. 16, Issue 8, pp. 933–947). Informa UK Limited. https://doi.org/10.1163/1568562054414658

[6] Cichowski K, Shih TS, Schmitt E, et al. Mouse Models of Tumor Development in Neurofibromatosis Type 1. Science. 1999;286(5447):2172-2176. doi:10.1126/science.286.5447.2172

Clausell-Tormos, J., Lieber, D., Baret, J.-C., El-Harrak, A., Miller, O. J., Frenz, L., Blouwolff, J., Humphry, K. J., Köster, S., Duan, H., Holtze, C., Weitz, D. A., Griffiths, A. D., & Merten, C. A. (2008). Droplet-Based Microfluidic Platforms for the Encapsulation and Screening of Mammalian Cells and Multicellular Organisms. In Chemistry & Biology (Vol. 15, Issue 5, pp. 427–437). Elsevier BV. https://doi.org/10.1016/j.chembiol.2008.04.004

[31] Crampton AL, Cummins KA, Wood DK. A High-Throughput Workflow to Study Remodeling of Extracellular Matrix-Based Microtissues. Tissue Engineering Part C: Methods. 2019;25(1):25-36. doi:10.1089/ten.tec.2018.0290

[32] Crampton AL, Cummins KA, Wood DK. A high-throughput microtissue platform to probe endothelial function in vitro. Integr Biol. 2018;10(9):555-565. doi:10.1039/C8IB00111A

Cummins, K. A., Bitterman, P. B., Tschumperlin, D. J., & Wood, D. K. (2021). A scalable 3D tissue culture pipeline to enable functional therapeutic screening for pulmonary fibrosis. *APL bioengineering*, *5*(4), 046102. https://doi.org/10.1063/5.0054967

Das, S., & Basu, B. (2019). An Overview of Hydrogel-Based Bioinks for 3D Bioprinting of Soft Tissues. In Journal of the Indian Institute of Science (Vol. 99, Issue 3, pp. 405–428). Springer Science and Business Media LLC. https://doi.org/10.1007/s41745-019-00129-5

[10] Dehner C, Moon CI, Zhang X, et al. Chromosome 8 gain is associated with high-grade transformation in MPNST. JCI Insight. 2021;6(6):e146351. doi:10.1172/jci.insight.146351

De Lora, J. A., Velasquez, J. L., Carroll, N. J., Freyer, J. P., & Shreve, A. P. (2020). Centrifugal Generation of Droplet-Based 3D Cell Cultures. In SLAS Technology (Vol. 25, Issue 5, pp. 436–445). Elsevier BV. https://doi.org/10.1177/2472630320915837

[39] Dodd RD, Mito JK, Eward WC, et al. NF1 Deletion Generates Multiple Subtypes of Soft-Tissue Sarcoma That Respond to MEK Inhibition. Mol Cancer Ther. 2013;12(9):1906-1917. doi:10.1158/1535-7163.MCT-13-0189

Dolega, M. E., Abeille, F., Picollet-D'hahan, N., & Gidrol, X. (2015). Controlled 3D culture in Matrigel microbeads to analyze clonal acinar development. In Biomaterials (Vol. 52, pp. 347–357). Elsevier BV. https://doi.org/10.1016/j.biomaterials.2015.02.042

[38] Dubois EA, Cohen AF. Trabectedin. British Journal of Clinical Pharmacology. 2009;68(3):320-321. doi:10.1111/j.1365-2125.2009.03490.x

Enck, K., Rajan, S.P., Aleman, J. *et al.* Design of an Adhesive Film-Based Microfluidic Device for Alginate Hydrogel-Based Cell Encapsulation. *Ann Biomed Eng* **48,** 1103–1111 (2020). https://doi.org/10.1007/s10439-020-02453-9

Fang, Y., & Eglen, R. M. (2017). Three-Dimensional Cell Cultures in Drug Discovery and Development. In SLAS Discovery (Vol. 22, Issue 5, pp. 456–472). Elsevier BV. https://doi.org/10.1177/1087057117696795

[22] Fernández-Rodríguez J, Creus-Bachiller E, Zhang X, et al. A high-throughput screening platform identifies novel combination treatments for Malignant Peripheral Nerve Sheath Tumors. Molecular Cancer Therapeutics. Published online May 5, 2022:molcanther.MCT-21-0947-A.2021. doi:10.1158/1535-7163.MCT-21-0947

Focaroli, S., Teti, G., Salvatore, V., Orienti, I., & Falconi, M. (2016). Calcium/Cobalt Alginate Beads as Functional Scaffolds for Cartilage Tissue Engineering. In Stem Cells International (Vol. 2016, pp. 1–12). Hindawi Limited. https://doi.org/10.1155/2016/2030478

German, Y., Vulliard, L., Kamnev, A., Pfajfer, L., Huemer, J., Mautner, A.-K., Rubio, A., Kalinichenko, A., Boztug, K., Ferrand, A., Menche, J., & Dupré, L. (2021). Morphological profiling of human T and NK lymphocytes by high-content cell imaging. In Cell Reports (Vol. 36, Issue 1, p. 109318). Elsevier BV. https://doi.org/10.1016/j.celrep.2021.109318

[42] Gosline SJC, Weinberg H, Knight P, et al. A high-throughput molecular data resource for cutaneous neurofibromas. Sci Data. 2017;4(1):170045. doi:10.1038/sdata.2017.45

Gupta, N., Liu, J. R., Patel, B., Solomon, D. E., Vaidya, B., & Gupta, V. (2016). Microfluidics-based 3D cell culture models: Utility in novel drug discovery and delivery research. In Bioengineering & Translational Medicine (Vol. 1, Issue 1, pp. 63–81). Wiley. https://doi.org/10.1002/btm2.10013

[7] Inoue A, Janke LJ, Gudenas BL, et al. A genetic mouse model with postnatal Nf1 and p53 loss recapitulates the histology and transcriptome of human malignant peripheral nerve sheath tumor. Neuro-Oncology Advances. 2021;3(1):vdab129. doi:10.1093/noajnl/vdab129

[19] Jacobi N, Seeboeck R, Hofmann E, et al. Organotypic three-dimensional cancer cell cultures mirror drug responses in vivo : lessons learned from the inhibition of EGFR signaling. Oncotarget. 2017;8(64):107423-107440. doi:10.18632/oncotarget.22475

Joshi, S., Mahadevan, G., Verma, S., & Valiyaveettil, S. (2020). Bioinspired adenine–dopamine immobilized polymer hydrogel adhesives for tissue engineering. In Chemical Communications (Vol. 56, Issue 76, pp. 11303–11306). Royal Society of Chemistry (RSC). https://doi.org/10.1039/d0cc04909c

[37] Kaplan HG, Rostad S, Ross JS, Ali SM, Millis SZ. Genomic Profiling in Patients With Malignant Peripheral Nerve Sheath Tumors Reveals Multiple Pathways With Targetable Mutations. J Natl Compr Canc Netw. 2018;16(8):967-974. doi:10.6004/jnccn.2018.7033

[11] Keng VW, Rahrmann EP, Watson AL, et al. PTEN and NF1 Inactivation in Schwann Cells Produces a Severe Phenotype in the Peripheral Nervous System That Promotes the Development and Malignant Progression of Peripheral Nerve Sheath Tumors. Cancer Res. 2012;72(13):3405-3413. doi:10.1158/0008-5472.CAN-11-4092

Kim, M. J., Chi, B. H., Yoo, J. J., Ju, Y. M., Whang, Y. M., & Chang, I. H. (2019). Structure establishment of three-dimensional (3D) cell culture printing model for bladder cancer. In J. W. Lee (Ed.), PLOS ONE (Vol. 14, Issue 10, p. e0223689). Public Library of Science (PLoS). https://doi.org/10.1371/journal.pone.0223689

[1] Kourea HP, Bilsky MH, Leung DHY, Lewis JJ, Woodruff JM. Subdiaphragmatic and intrathoracic paraspinal malignant peripheral nerve sheath tumors: A clinicopathologic study of 25 patients and 26 tumors. Cancer. 1998;82(11):2191-2203. doi:10.1002/(SICI)1097-0142(19980601)82:11<2191::AID-CNCR14>3.0.CO;2-P

Krüger, A. J. D., Bakirman, O., Guerzoni, Luis. P. B., Jans, A., Gehlen, D. B., Rommel, D., Haraszti, T., Kuehne, A. J. C., & De Laporte, L. (2019). Compartmentalized Jet Polymerization as a High-Resolution Process to Continuously Produce Anisometric Microgel Rods with Adjustable Size and Stiffness. In Advanced Materials (Vol. 31, Issue 49, p. 1903668). Wiley. https://doi.org/10.1002/adma.201903668

Lee, D., Pathak, S. & Jeong, JH. Design and manufacture of 3D cell culture plate for mass production of cell-spheroids. *Sci Rep* **9,** 13976 (2019). https://doi.org/10.1038/s41598-019-50186-0

[9] Lee W, Teckie S, Wiesner T, et al. PRC2 is recurrently inactivated through EED or SUZ12 loss in malignant peripheral nerve sheath tumors. Nat Genet.

2014;46(11):1227-1232. doi:10.1038/ng.3095

[26] Li H. Aligning sequence reads, clone sequences and assembly contigs with BWA-MEM. arXiv:13033997 [q-bio]. Published online May 26, 2013. Accessed January 25, 2022. http://arxiv.org/abs/1303.3997

Li, J., Wang, Q., Gu, Y., Zhu, Y., Chen, L., & Chen, Y. (2017). Production of Composite Scaffold Containing Silk Fibroin, Chitosan, and Gelatin for 3D Cell Culture and Bone Tissue Regeneration. In Medical Science Monitor (Vol. 23, pp. 5311–5320). International Scientific Information, Inc. https://doi.org/10.12659/msm.905085

[16] Li S, Shen D, Shao J, et al. Endocrine-Therapy-Resistant ESR1 Variants Revealed by Genomic Characterization of Breast-Cancer-Derived Xenografts. Cell Reports. 2013;4(6):1116-1130. doi:10.1016/j.celrep.2013.08.022

Li, X. (James), Valadez, A. V., Zuo, P., & Nie, Z. (2012). Microfluidic 3D cell culture: potential application for tissue-based bioassays. In Bioanalysis (Vol. 4, Issue 12, pp. 1509–1525). Future Science Ltd. https://doi.org/10.4155/bio.12.133

Liao, C., Wuethrich, A., & Trau, M. (2020). A material odyssey for 3D nano/microstructures: two photon polymerization based nanolithography in bioapplications. In Applied Materials Today (Vol. 19, p. 100635). Elsevier BV. https://doi.org/10.1016/j.apmt.2020.100635

[30] Love MI, Huber W, Anders S. Moderated estimation of fold change and dispersion for RNA-seq data with DESeq2. Genome Biol. 2014;15(12):550. doi:10.1186/s13059-014-0550-8

Macosko, E. Z., Basu, A., Satija, R., Nemesh, J., Shekhar, K., Goldman, M., Tirosh, I., Bialas, A. R., Kamitaki, N., Martersteck, E. M., Trombetta, J. J., Weitz, D. A., Sanes, J. R., Shalek, A. K., Regev, A., & McCarroll, S. A. (2015). Highly Parallel Genome-wide Expression Profiling of Individual Cells Using Nanoliter Droplets. In Cell (Vol. 161, Issue 5, pp. 1202–1214). Elsevier BV. https://doi.org/10.1016/j.cell.2015.05.002

[17] Magallon-Lorenz M, Terribas E, Fernández M, et al. A detailed landscape of genomic alterations in malignant peripheral nerve sheath tumor cell lines challenges the current MPNST diagnosis. :38.

[34] Matsuyama T, Ishikawa T, Mogushi K, et al. MUC12 mRNA expression is an independent marker of prognosis in stage II and stage III colorectal cancer. Int J Cancer. 2010;127(10):2292-2299. doi:10.1002/ijc.25256

[28] Mayakonda A, Lin DC, Assenov Y, Plass C, Koeffler HP. Maftools: efficient and comprehensive analysis of somatic variants in cancer. Genome Res. 2018;28(11):1747-1756. doi:10.1101/gr.239244.118

[27] McLaren W, Gil L, Hunt SE, et al. The Ensembl Variant Effect Predictor. Genome Biol. 2016;17(1):122. doi:10.1186/s13059-016-0974-4

Mohamed, M. G. A., Kheiri, S., Islam, S., Kumar, H., Yang, A., & Kim, K. (2019). An

integrated microfluidic flow-focusing platform for on-chip fabrication and filtration of cell-laden microgels. In Lab on a Chip (Vol. 19, Issue 9, pp. 1621–1632). Royal Society of Chemistry (RSC). https://doi.org/10.1039/c9lc00073a

[40] Nissan MH, Pratilas CA, Jones AM, et al. Loss of NF1 in Cutaneous Melanoma Is Associated with RAS Activation and MEK Dependence. Cancer Res. 2014;74(8):2340-2350. doi:10.1158/0008-5472.CAN-13-2625

Ong, S.-M., Zhang, C., Toh, Y.-C., Kim, S. H., Foo, H. L., Tan, C. H., van Noort, D., Park, S., & Yu, H. (2008). A gel-free 3D microfluidic cell culture system. In Biomaterials (Vol. 29, Issue 22, pp. 3237–3244). Elsevier BV. https://doi.org/10.1016/j.biomaterials.2008.04.022

[21] Oyama R, Kito F, Takahashi M, et al. Establishment and characterization of patient-derived cancer models of malignant peripheral nerve sheath tumors. Cancer Cell Int. 2020;20(1):58. doi:10.1186/s12935-020-1128-z

[29] Patro R, Duggal G, Love MI, Irizarry RA, Kingsford C. Salmon provides fast and bias-aware quantification of transcript expression. Nat Methods. 2017;14(4):417-419. doi:10.1038/nmeth.4197

[36] Peille AL, Vuaroqueaux V, Wong SS, et al. Evaluation of molecular subtypes and clonal selection during establishment of patient-derived tumor xenografts from gastric adenocarcinoma. Commun Biol. 2020;3(1):367. doi:10.1038/s42003-020-1077-z

Peirone, M., Ross, C. J. D., Hortelano, G., Brash, J. L., & Chang, P. L. (1998). Encapsulation of various recombinant mammalian cell types in different alginate microcapsules. In Journal of Biomedical Materials Research (Vol. 42, Issue 4, pp. 587–596). Wiley. https://doi.org/10.1002/(sici)1097-4636(19981215)42:4<587::aid-jbm15>3.0.co;2-x

[8] Pemov A, Hansen NF, Sindiri S, et al. Low mutation burden and frequent loss of CDKN2A/B and SMARCA2, but not PRC2, define premalignant neurofibromatosis type 1–associated atypical neurofibromas. Neuro-Oncology. 2019;21(8):981-992. doi:10.1093/neuonc/noz028

[23] Pollard K, Banerjee J, Doan X, et al. A clinically and genomically annotated nerve sheath tumor biospecimen repository. Sci Data. 2020;7(1):184. doi:10.1038/s41597-020-0508-5

[3] Prudner BC, Ball T, Rathore R, Hirbe AC. Diagnosis and management of malignant peripheral nerve sheath tumors: Current practice and future perspectives. Neuro-Oncology Advances. 2020;2(Supplement_1):i40-i49. doi:10.1093/noajnl/vdz047

Jang, M., Yang, S. & Kim, P. Microdroplet-based cell culture models and their application. *BioChip J* **10,** 310–317 (2016). https://doi.org/10.1007/s13206-016-0407-1

Joshi, P., Datar, A., Yu, K.-N., Kang, S.-Y., & Lee, M.-Y. (2018). High-content imaging assays on a miniaturized 3D cell culture platform. In Toxicology in Vitro (Vol. 50, pp. 147–159). Elsevier BV. https://doi.org/10.1016/j.tiv.2018.02.014

[18] Kim J, Koo BK, Knoblich JA. Human organoids: model systems for human biology and medicine. Nat Rev Mol Cell Biol. 2020;21(10):571-584. doi:10.1038/s41580-020-0259-3

[14] Koga Y, Ochiai A. Systematic Review of Patient-Derived Xenograft Models for Preclinical Studies of Anti-Cancer Drugs in Solid Tumors. Cells. 2019;8(5):418. doi:10.3390/cells8050418

[46] Raghavan S, Winter PS, Navia AW, et al. Microenvironment drives cell state, plasticity, and drug response in pancreatic cancer. Cell. 2021;184(25):6119-6137.e26. doi:10.1016/j.cell.2021.11.017

[12] Rahrmann EP, Watson AL, Keng VW, et al. Forward genetic screen for malignant peripheral nerve sheath tumor formation identifies new genes and pathways driving tumorigenesis. Nat Genet. 2013;45(7):756-766. doi:10.1038/ng.2641

Rashid, S. T., Corbineau, S., Hannan, N., Marciniak, S. J., Miranda, E., Alexander, G., Huang-Doran, I., Griffin, J., Ahrlund-Richter, L., Skepper, J., Semple, R., Weber, A., Lomas, D. A., & Vallier, L. (2010). Modeling inherited metabolic disorders of the liver using human induced pluripotent stem cells. In Journal of Clinical Investigation (Vol. 120, Issue 9, pp. 3127–3136). American Society for Clinical Investigation. https://doi.org/10.1172/jci43122

[2] Reilly KM, Kim A, Blakely J, et al. Neurofibromatosis Type 1–Associated MPNST State of the Science: Outlining a Research Agenda for the Future. JNCI: Journal of the National Cancer Institute. 2017;109(8). doi:10.1093/jnci/djx124

[43] Richter-Pechańska P, Kunz JB, Bornhauser B, et al. PDX models recapitulate the genetic and epigenetic landscape of pediatric T-cell leukemia. EMBO Mol Med. 2018;10(12). doi:10.15252/emmm.201809443

[41] Rodrigues J, Heinrich MA, Teixeira LM, Prakash J. 3D In Vitro Model (R)evolution: Unveiling Tumor–Stroma Interactions. Trends in Cancer. 2021;7(3):249-264. doi:10.1016/j.trecan.2020.10.009

[20] Roy V, Magne B, Vaillancourt-Audet M, et al. Human Organ-Specific 3D Cancer Models Produced by the Stromal Self-Assembly Method of Tissue Engineering for the Study of Solid Tumors. BioMed Research International. 2020;2020:1-23. doi:10.1155/2020/6051210

Scannell, J. W., & Bosley, J. (2016). When Quality Beats Quantity: Decision Theory, Drug Discovery, and the Reproducibility Crisis. In M. Gasparini (Ed.), PLOS ONE (Vol. 11, Issue 2, p. e0147215). Public Library of Science (PLoS). https://doi.org/10.1371/journal.pone.0147215

Seng Ng, S., Saeb-Parsy, K., Segal, J. M., Serra, M. P., Blackford, S. J. I., Lopez, M. H., No, D. Y., Frank, C. W., Cho, N. J., Nakauchi, H., Glenn, J. S., & Rashid, S. T. (2018). Conversion of iPS derived hepatic progenitors into scalable, functional and developmentally relevant human organoids using an inverted colloidal crystal poly (ethylene glycol) scaffold engineered from collagen-coated pores of defined size. Cold Spring Harbor Laboratory. https://doi.org/10.1101/296327

Shao, C., Liu, Y., Chi, J., Wang, J., Zhao, Z., & Zhao, Y. (2019). Responsive Inverse Opal Scaffolds with Biomimetic Enrichment Capability for Cell Culture. In Research (Vol. 2019, pp. 1–10). American Association for the Advancement of Science (AAAS). https://doi.org/10.34133/2019/9783793

Slaughter, B. V., Khurshid, S. S., Fisher, O. Z., Khademhosseini, A., & Peppas, N. A. (2009). Hydrogels in Regenerative Medicine. In Advanced Materials (Vol. 21, Issues 32–33, pp. 3307–3329). Wiley. https://doi.org/10.1002/adma.200802106

Srinivasan, S., Jayasree, R., Chennazhi, K. P., Nair, S. V., & Jayakumar, R. (2012). Biocompatible alginate/nano bioactive glass ceramic composite scaffolds for periodontal tissue regeneration. In Carbohydrate Polymers (Vol. 87, Issue 1, pp. 274–283). Elsevier BV. https://doi.org/10.1016/j.carbpol.2011.07.058

Sutherland, R. M., McCredie, J. A., and Inch, W. R. (1971). Growth of multicell spheroids in tissue culture as a model of nodular carcinomas. *J. Natl. Cancer Inst.* 46, 113–120.

[15] Tignanelli CJ, Loeza SGH, Yeh JJ. KRAS and PIK3CA mutation frequencies in patient derived xenograft (PDX) models of pancreatic and colorectal cancer are reflective of patient tumors and stable across passages. Published online 2015:11.

Utama, R. H., Tan, V. T. G., Tjandra, K. C., Sexton, A., Nguyen, D. H. T., O'Mahony, A. P., Du, E. Y., Tian, P., Ribeiro, J. C. C., Kavallaris, M., & Gooding, J. J. (2021). A Covalently Crosslinked Ink for Multimaterials Drop-on-Demand 3D Bioprinting of 3D Cell Cultures. In Macromolecular Bioscience (Vol. 21, Issue 9, p. 2100125). Wiley. https://doi.org/10.1002/mabi.202100125

[13] Vélez-Reyes GL, Koes N, Ryu JH, et al. Transposon Mutagenesis-Guided CRISPR/Cas9 Screening Strongly Implicates Dysregulation of Hippo/YAP Signaling in Malignant Peripheral Nerve Sheath Tumor Development. Cancers. 2021;13(7):1584. doi:10.3390/cancers13071584

Wang, Y., Huang, X., Shen, Y., Hang, R., Zhang, X., Wang, Y., Yao, X., & Tang, B. (2019). Direct writing alginate bioink inside pre-polymers of hydrogels to create patterned vascular networks. In Journal of Materials Science (Vol. 54, Issue 10, pp. 7883–7892). Springer Science and Business Media LLC. https://doi.org/10.1007/s10853-019-03447-2

[24] Wang J, Pollard K, Allen AN, et al. Combined Inhibition of SHP2 and MEK Is Effective in Models of NF1-Deficient Malignant Peripheral Nerve Sheath Tumors. Cancer Res. 2020;80(23):5367-5379. doi:10.1158/0008-5472.CAN-20-1365

Xu, J., Qi, G., Sui, C., Wang, W., & Sun, X. (2019). 3D h9e peptide hydrogel: An advanced three-dimensional cell culture system for anticancer prescreening of chemopreventive phenolic agents. In Toxicology in Vitro (Vol. 61, p. 104599). Elsevier BV. https://doi.org/10.1016/j.tiv.2019.104599

[5] Yang FC, Ingram DA, Chen S, et al. Nf1-Dependent Tumors Require a Microenvironment Containing Nf1+/−- and c-kit-Dependent Bone Marrow. Cell. 2008;135(3):437-448. doi:10.1016/j.cell.2008.08.041

Y. Yang, H. Wu, J. Jia and P. -O. Bagnaninchi, "Scaffold-Based 3-D Cell Culture Imaging Using a Miniature Electrical Impedance Tomography Sensor," in *IEEE Sensors Journal*, vol. 19, no. 20, pp. 9071-9080, 15 Oct.15, 2019, doi: 10.1109/JSEN.2019.2924154.

[35] Yoo SM, Cerione RA, Antonyak MA. The Arf-GAP and protein scaffold Cat1/Git1 as a multifaceted regulator of cancer progression. Small GTPases. 2020;11(2):77-85. doi:10.1080/21541248.2017.1362496

Zhang, C., Zhao, Z., Abdul Rahim, N. A., van Noort, D., & Yu, H. (2009). Towards a human-on-chip: Culturing multiple cell types on a chip with compartmentalized microenvironments. In Lab on a Chip (Vol. 9, Issue 22, p. 3185). Royal Society of Chemistry (RSC). https://doi.org/10.1039/b915147h

[4] Zheng H, Chang L, Patel N, et al. Induction of Abnormal Proliferation by Nonmyelinating Schwann Cells Triggers Neurofibroma Formation. Cancer Cell. 2008;13(2):117-128. doi:10.1016/j.ccr.2008.01.002